Biosensors and Bioelectronics 98 (2017) 478–485

Contents lists available at ScienceDirect

Biosensors and Bioelectronics

journal homepage: www.elsevier.com/locate/bios

Pen-on-paper strategy for point-of-care testing: Rapid prototyping of fully written microfluidic biosensor

Zedong Li[a,b], Fei Li[a,b,*], Yue Xing[b,c], Zhi Liu[b,d], Minli You[a,b], Yingchun Li[a,b], Ting Wen[e], Zhiguo Qu[d], Xiao Ling Li[f], Feng Xu[a,b]

[a] The Key Laboratory of Biomedical Information Engineering of Ministry of Education, School of Life Science and Technology, Xi'an Jiaotong University, Xi'an 710049, PR China
[b] Bioinspired Engineering and Biomechanics Center (BEBC), Xi'an Jiaotong University, Xi'an 710049, PR China
[c] School of Energy and Power Engineering, Xi'an Jiaotong University, Xi'an 710049, PR China
[d] Key Laboratory of Thermo-Fluid Science and Engineering of Ministry of Education, School of Energy and Power Engineering, Xi'an Jiaotong University, Xi'an 710049, PR China
[e] Xi'an Diandi Biotech Company, Xi'an 710049, PR China
[f] School of Mechanical Engineering, Xi'an Jiaotong University, Xi'an 710049, PR China

ARTICLE INFO

Keywords:
Point-of-care testing
Paper microfluidics
Biosensor
Writing
Wax pen
Ink pen

ABSTRACT

Paper-based microfluidic biosensors have recently attracted increasing attentions in point-of-care testing (POCT) territories benefiting from their affordable, accessible and eco-friendly features, where technologies for fabricating such biosensors are preferred to be equipment free, easy-to-operate and capable of rapid prototyping. In this work, we developed a pen-on-paper (PoP) strategy based on two custom-made pens, *i.e.*, a wax pen and a conductive-ink pen, to fully write paper-based microfluidic biosensors through directly writing both microfluidic channels and electrodes. Particularly, the proposed wax pen is competent to realize one-step fabrication of wax channels on paper, as the melted wax penetrates into paper during writing process without any post-treatments. The practical applications of the fabricated paper-based microfluidic biosensors are demonstrated by both colorimetric detection of *Salmonella typhimurium DNA* with detection limit of 1 nM and electrochemical measurement of glucose with detection limit of 1 mM. The developed PoP strategy for making microfluidic biosensors on paper characterized by true simplicity, prominent portability and excellent capability for rapid prototyping shows promising prospect in POCT applications.

1. Introduction

Paper has extended its application from traditional information recording and package functions in our daily life to more recently microfluidic biosensors for point-of-care testing (POCT), due to its specific properties of hydrophilicity, flexibility, porosity, portability and disposability (Cate et al., 2014; Ge et al., 2012; Hu et al., 2014; Martinez et al., 2008, 2009; Pardee et al., 2016). To date, paper-based microfluidic POCT biosensors, mostly based on colorimetric assays with easy readout and electrochemical assays with improved sensitivity and quantitative readout (Dungchai et al., 2009; Martinez et al., 2007, 2008; Maxwell et al., 2013; Nie et al., 2010a; Zang et al., 2012), have found widespread applications in human health diagnosis (Klasner et al., 2010; Martinez et al., 2007), environment monitoring (Apilux et al., 2010; Wang et al., 2009) and food quality control (Hossain et al., 2009). For instance, a paper-based microfluidic colorimetric sensor has been developed for detecting multiple heavy metal ions (*e.g.*, Hg^{2+}, Cu^{2+} and Cr^{6+}) in tap water (Hossain and Brennan, 2011). A paper-based microfluidic electrochemical biosensor has been developed for quantitatively detecting human health related targets (*e.g.*, glucose and lactate) with the participation of an electronic reader (Nie et al., 2010a, 2010b). *More recently, an aptamer-based colorimetric biosensor has also been created for achieving naked eye quantitative assay on paper, which relies on measuring the length of color change region or counting the number of color change zones (*Zhang et al., 2016*).* For these applications, the ideal paper-based microfluidic biosensors should be affordable, portable, easy to use, rapid, user friendly and capable of rapid prototyping.

Two essential steps are generally involved to construct paper-based microfluidic biosensors, *i.e.*, fabrication of microfluidic channels on

* Corresponding author at: The Key Laboratory of Biomedical Information Engineering of Ministry of Education, School of Life Science and Technology, Xi'an Jiaotong University, Xi'an 710049, PR China.
E-mail address: feili@mail.xjtu.edu.cn (F. Li).

http://dx.doi.org/10.1016/j.bios.2017.06.061
Received 22 March 2017; Received in revised form 10 June 2017; Accepted 28 June 2017
Available online 01 July 2017
0956-5663/

paper for guiding sample flow and construction of sensing elements on paper for identifying and detecting target species in sample. To fabricate microfluidic channels on paper, an effective way is patterning hydrophobic barriers on paper to define hydrophilic channels (Li et al., 2012). Various methods have been developed to pattern hydrophobic barriers on paper, which can be classified into chemical methods (*e.g.*, photolithography (Martinez et al., 2007), inkjet etching (Abe et al., 2008) and plasma treatment (Li et al., 2008)) and physical methods (*e.g.*, cutting (Fenton et al., 2008), plotting (Bruzewicz et al., 2008), contact-printing (Dornelas et al., 2015) and wax patterning (Carrilho et al., 2009; Nilghaz et al., 2012; Renault et al., 2014b)). The chemical methods offer high spatial resolution, but involve complicated fabrication process, expensive equipment and harmful chemicals. In addition, the treatment process on paper by chemicals may damage paper properties, and chemical residuals on paper may disturb detection results. In comparison, the physical methods featured by chemicals free and reduced fabrication steps are much simpler and more environmental friendly. *For example, permanent markers have been employed for one-step construction of hydrophobic resin barriers on paper (*Nie et al., 2012*).* Furthermore, wax patterning on paper, as the most commonly used physical method with the advantages of simplicity, accessibility and low cost, can be achieved through printing (Carrilho et al., 2009), pencil writing (Lu et al., 2009), screen printing (Dungchai et al., 2011) and dipping (Songjaroen et al., 2011). But there are several limitations associated with these existing wax patterning methods. For instance, it is difficult to produce precise pattern with high resolution using wax pencil writing, while wax printing method requires a costly wax printer instrument, limiting its wide accessibility. Besides, for formation of complete hydrophobic barriers on paper, an extra step of heating (normally using a hot plate) is needed to melt solid-phase wax to penetrate into paper, which makes it challenging to well control the resolution of fabricated paper-based microfluidics. Moreover, these methods are neither portable nor rapid for making prototype systems, thus not ideal for POCT applications especially at resource limited settings. Hence, there is still an unmet need for a fabrication method to make wax-based microfluidic channels on paper with minimized cost, simplified process, improved portability and rapid prototype process.

For construction of sensing elements on paper, the recently developed pen-based writing method has emerged as an alternative to the conventional methods (*e.g.* screen printing (Nie et al., 2010b; Renault et al., 2014a) and inkjet printing (Määttänen et al., 2013)) owing to the good compatibility with paper, the instrument-free property and the rapid prototyping capability (Bandodkar et al., 2015; Dossi et al., 2014; Li et al., 2015; Russo et al., 2011). For example, a ball pen filled with an enzymatic ink composed of graphite powder and enzyme has been used to directly write electrodes on human skin with the merit of eliminating additional sensor modification steps and endowing the user sufficient freedom to make do-it-yourself (DIY) biosensors (Bandodkar et al., 2015). A pressure-assisted ball pen has been utilized to write viscous conductive inks as electrodes of paper-based electrochemical POCT devices (Li et al., 2015). But as far as we know, construction of both microfluidic channels and electrochemical sensing elements fully using the pen-based writing strategy has not been reported yet.

In this work, we developed a pen-on-paper (PoP) strategy for fabrication of paper-based microfluidic biosensors through direct writing both microfluidic channels and electrochemical detection unit on paper using two custom-designed pens, as schematically shown in Fig. 1. Firstly, a wax pen and a conductive-ink pen were custom-designed and fabricated. And these two pens were used to write wax barriers as microfluidic channels and carbon electrodes as electrochemical detection unit on paper to form fully written paper-based microfluidic biosensors. Then the rapid-prototyped paper-based biosensors were applied in POCT field, demonstrated *via* two examples, *i.e.*, colorimetric detection of *Salmonella typhimurium DNA* on a paper

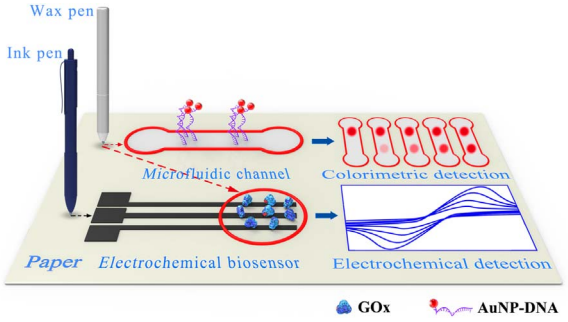

Fig. 1. Schematic illustration of the pen-on-paper strategy for rapid prototyping of fully written microfluidic biosensors for both colorimetric and electrochemical detection in POCT applications.

"notebook" platform and electrochemical measurement of glucose on paper.

2. Experimental section

2.1. Materials

Carbon ink (Electrodage 423ss) and diluent (SBJ-5) were purchased from Acheson (USA). Solid wax, ball pen (ball size of 1.0 mm), heating wire, power adapter (12 V output) and the spring for construction of the paper "notebook" platform were purchased from local stores. Filter papers (qualitative, 102, 15 mm) and nitrocellulose (NC) membranes were obtained from Hangzhou Whatman-Xinhua Filter Paper Co., Ltd (China) and Shanghai Jiening Biotech Co., Ltd., respectively. Poly(methyl methacrylate) (PMMA) boards were obtained from Legend Technology Ltd. (China). Ferrocene methanol (FcMeOH), potassium ferrocyanide ($K_3Fe(CN)_6$), sodium chloride (NaCl), phosphate buffer (PBS) and saline sodium citrate (SSC) buffer are all of analytical grade and obtained from Sigma-Aldrich. D-(+)-glucose and glucose oxidase (GOx) (10 KU) were obtained from MP Biomedlcals, LLC (France). Human serum (168014) was obtained from Zhongkechenyu (Beijing) Biotech Co., Ltd. Gold nanoparticles (AuNPs) with diameter of 13 nm were synthesized according to the protocol described in our previous work (Tang et al., 2016). All aqueous solutions used in this work were prepared from Milli-Q reagent water (Millipore Corp., resistivity of > 18.2 MΩ cm at 25 °C).

2.2. Design and fabrication of wax pen and conductive-ink pen

The wax pen used in this work was an assembly of a ball pen filled with wax and a heating unit, as illustrated in Fig. 2a. Firstly, the ball pen was pre-emptied and cleaned by water and dried at room temperature prior to use. The liquid melted wax was loaded into the empty ball pen through pipetting. Then the ball pen was inserted into a customized conducting tube, outside of which an insulating heating wire was closely twined for uniformly transferring heat from the heating resource (*i.e.*, wire) to the wax in the ball pen. The heating wire was connected with a power adapter as a power supply and a thermostatic controller for temperature control. A custom-designed holder finally encompassed the conducting tube for easy operation of end-users. The conducting tube and the holder were both made of aluminum based on its good thermal conductivity and light-weight property. The fabrication of the conductive-ink pen was similar to that of the wax pen using a diluted carbon ink, which was the mixture of the carbon ink and the diluent with the mass ratio of 1.0: 0.6. *This newly developed ink pen holds simpler configuration in comparison to the pressure-assisted ball pen developed in our previous work (*Li et al., 2015*), as it can be directly applied to writing electrodes on paper by diluting the conductive ink (i.e., carbon ink) inside the pen prior to use without need for any extra pressure-assisted device.*

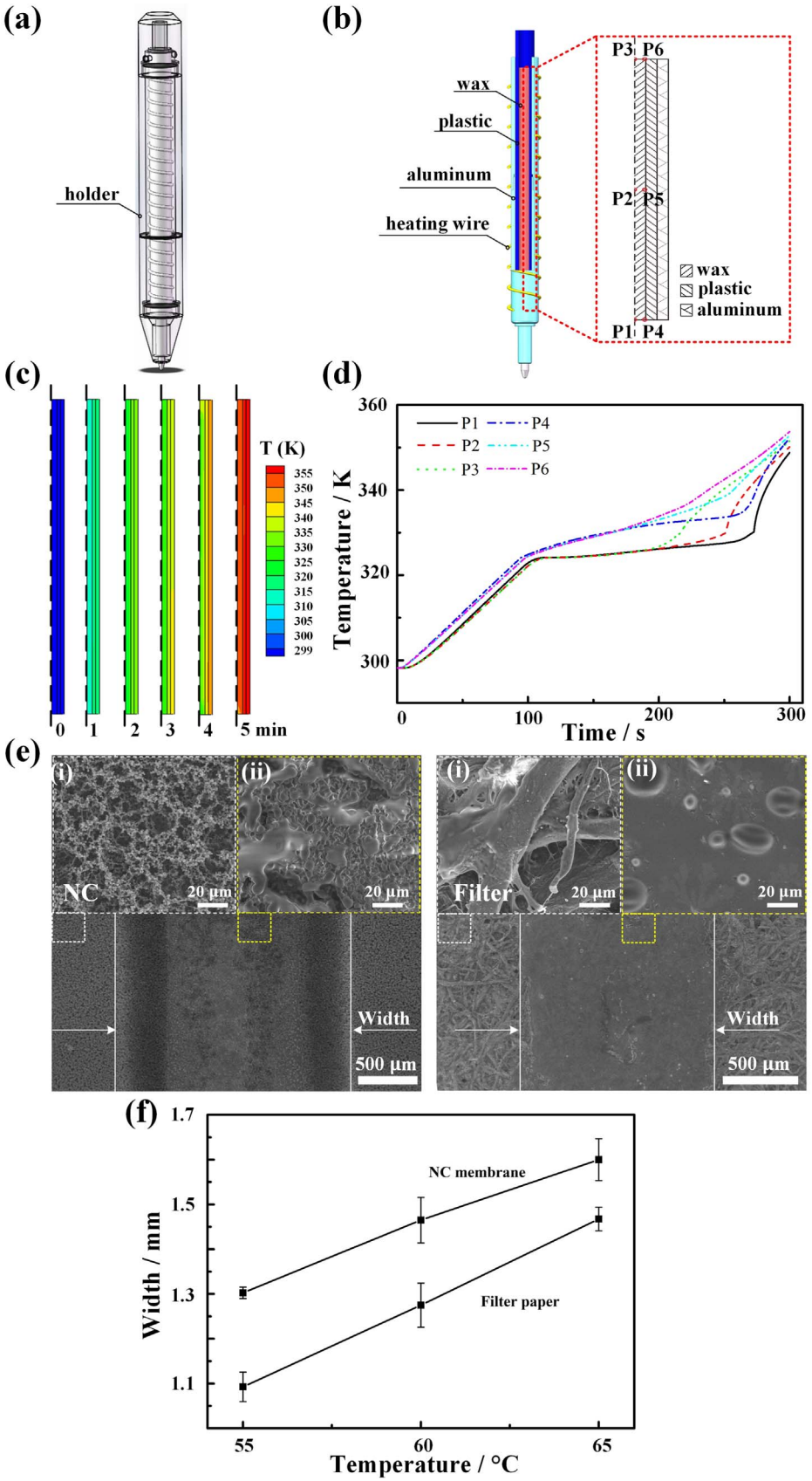

Fig. 2. Characterizations of the wax pen and the written wax patterns on paper. (a) Scheme structure of the wax pen. (b) The inner structure of the pen and its cross section. (c) The temperature contour of the axisymmetric section in the heating process. (d) Temperatures at different positions of ball pen as a function of time. (e) SEM images of the wax patterns written on a NC membrane (left) and a filter paper (right), (i) the blank paper and (ii) the wax coated paper. (f) The relationship between the width of the wax lines written on a NC membrane and a filter paper and the wax temperature.

2.3. Heat transfer model of wax pen

To better optimize the energy control during writing wax on paper using the developed wax pen, we established a physical model including three layers (*i.e.*, aluminum, plastic and wax) to investigate the heat transfer and the melting process of wax in the heating cylinder (Fig. 2b). For simplification, the inner heating cylinder, twined and heated by the heating wire, was considered as the main part for simulation. In this work, we assumed that the wax is an isotropic and homogeneous phase change material (PCM), and the melting wax is considered as a Newtonian incompressible liquid. To evaluate the changing density of the melting wax in the buoyancy lift of natural convection liquid, the Boussinesq approximation was adopted in the physical model. Based on these assumptions. The governing equations of the solid-liquid two-phase heat transfer include continuity (1), momentum (2, 3) and energy Eq. (4) (Mustaffar et al., 2015):

$$\mathrm{div}(\rho\vec{u}) = 0 \tag{1}$$

$$\frac{\partial(\rho\vec{u})}{\partial t} + \nabla\cdot(\rho\vec{u}u) = \nabla\cdot(\mu \mathrm{grad}u) - \frac{\partial P}{\partial x} + S_x \tag{2}$$

$$\frac{\partial(\rho\vec{u})}{\partial t} + \nabla\cdot(\rho\vec{u}v) = \nabla\cdot(\mu \mathrm{grad}v) - \frac{\partial P}{\partial y} - \rho g + S_y \tag{3}$$

$$\frac{\partial(\rho H)}{\partial t} + \frac{\partial(\rho \Delta H)}{\partial t} + \nabla\cdot(\rho\vec{u}\mathrm{H}) = \nabla\cdot(\lambda\nabla T) \tag{4}$$

where ρ= density, $\vec{u}$ = liquid velocity, P= pressure, μ= viscosity, g = gravitational acceleration, λ = thermal conductivity, T = temperature and H= total enthalpy. The source terms S_x and S_y are determined by the Darcy's damping law, as illustrated in Mustaffar's work (Mustaffar et al., 2015). Besides, H consists of the liquid-phase latent enthalpy ΔH and specific enthalpy h, defining as $H = \Delta H + h$. In the phase change process, ΔH depends on the liquid fraction $f(T)$ and varies from 0 (solid) to1 (liquid). Thus, the liquid-phase fraction can be expressed as follows,

$$f(T) = \begin{cases} 0 & , T < T_{solid} \\ \frac{T - T_{solid}}{T_{liquid} - T_{solid}} & , T_{solid} < T < T_{liquid} \\ 1 & , T > T_{liquid} \end{cases} \tag{5}$$

For the aluminum and plastic cylinder, the energy equation can be expressed as

$$\frac{\partial(\rho c_p T)}{\partial t} = \nabla\cdot(\lambda\nabla T) \tag{6}$$

where c_p is the specific heat. The geometrical and physical parameters of each cylinder were additionally presented in Table S1. At the initial state, the room temperature of 298.15 K was selected to be the starting temperature. During heating, a constant heat flux of 2630 W m^{-2}, as calculated according to the power of the heating wire, is delivered to the aluminum cylinder surface. Considering that the heating cylinder is axisymmetric, we simply constructed a half of cross section of the ball pen with uniform grid using GAMBIT software, while the mathematical thermal modeling was dealt by using the Solidification/Melting module in the FLUENT solver.

2.4. Fully written paper-based microfluidic biosensors using the PoP strategy

To construct the paper-based microfluidic biosensors, the developed wax pen and conductive-ink pen were utilized to write microfluidic channel and electrochemical detection unit on paper, respectively. For the wax pen, the heating temperature for melting wax was set firstly. When the temperature reached the melting point of wax, the wax in the ball pen melted and flowed out of the ball pen tip when contacting the paper surface. Then the liquid wax penetrated into the paper through the entire thickness of the paper during writing and solidified after cooling at room temperature. Simple straight wax lines and more complex wax patterns were written using a ruler and customized PMMA masks, respectively. The written hydrophobic wax lines finally formed the microfluidic channels on paper.

Following the protocol described in our previous report (Li et al., 2015), the electrochemical detection system, composed of a carbon working electrode, a counter electrode and a quasi-reference electrode, was directly written on a filter paper using the carbon ink pen guided by a ruler. Then the paper written with carbon inks was cured in oven at 70 °C for 30 min to form the final carbon electrodes on paper. Subsequently, circular microfluidic channel surrounding the electrodes was written using the wax pen.

2.5. Fabrication of the paper "notebook" platform

For fabrication of the paper-based colorimetric platform, the paper "notebook" design was created. As demonstrated in Fig. 4, the paper "notebook" platform was fabricated by hinging two layers (*i.e.*, top layer and bottom layer) together using a spring. The top layer consisted of a PMMA sheet with a sample inlet hole, an immersing pad and an absorbent pad, which were designed with Corel Draw X3 software and cut by a laser cutter (Versa LASER VLS3.50). The PMMA sheet was introduced because of its high transparency, enabling end users the ability to track the fluid flow and easily observe detection results. The immersing pad adhered on the PMMA can provide the zone for immobilization of AuNPs, while the absorbent pad can offer the driving force to transfer liquid along the microfluidic channels through capillary force. The bottom layer consisted of a NC membrane containing a microfluidic channel used for modification of capture probe and control probe for the assay reaction and a supporting pad for offering mechanical support to the platform. After stacking the two layers along with the spring, the immersing pad and the absorbent pad on the top layer closely contacted both ends of the channel on the bottom layer ascribed to the gravity action from the top layer, finally forming a daily notebook-structured paper-based colorimetric platform. Prior to use, 8 μL solution containing detection probes conjugated AuNPs (AuNP-DPs) was spotted on the immersing pad. Subsequently, 0.5 μL of capture probes and control probes solutions were spotted into the microfluidic channel, respectively. Then the platform was placed in an oven at the temperature of 37 °C for drying. The AuNP-DPs solution, capture probes solution and control probes solution were prepared referring to our previously published protocol (Tang et al., 2017).

2.6. Electrochemical measurements

Cyclic voltammetric (CV) and chronoamperometric measurements were both performed on a CHI852D electrochemical workstation (Chenhua Instrument Ltd., China). CV measurements were carried out in an aqueous solution containing 1.0 mM FcMeOH and 0.1 M NaCl with scanning potential from −600 to 600 mV at various scan rates (10, 20, 50, 75 and 100 mV s^{-1}). For electrochemical detection of glucose, the electrode surfaces of the paper-based electrochemical biosensor were modified through spotting 10 μL PBS solutions (pH = 7.4) containing 250 mM $K_3Fe(CN)_6$ and 500 U/ml GOx. The chronoamperometric measurements were carried out with applying a constant potential of 400 mV for 200 s in the spiked serum containing different concentrations of glucose.

2.7. Samples for detection

The target DNA and probes of Salmonella typhimurium were synthesized and provided from Sangon Biotech Co., Ltd (Shanghai, China). And the detailed sequences are shown in Table S2. *The Salmonella typhimurium samples involved in colorimetric detection, with concentrations of 1, 5, 20, 50 and 100 nM, were prepared by diluting the*

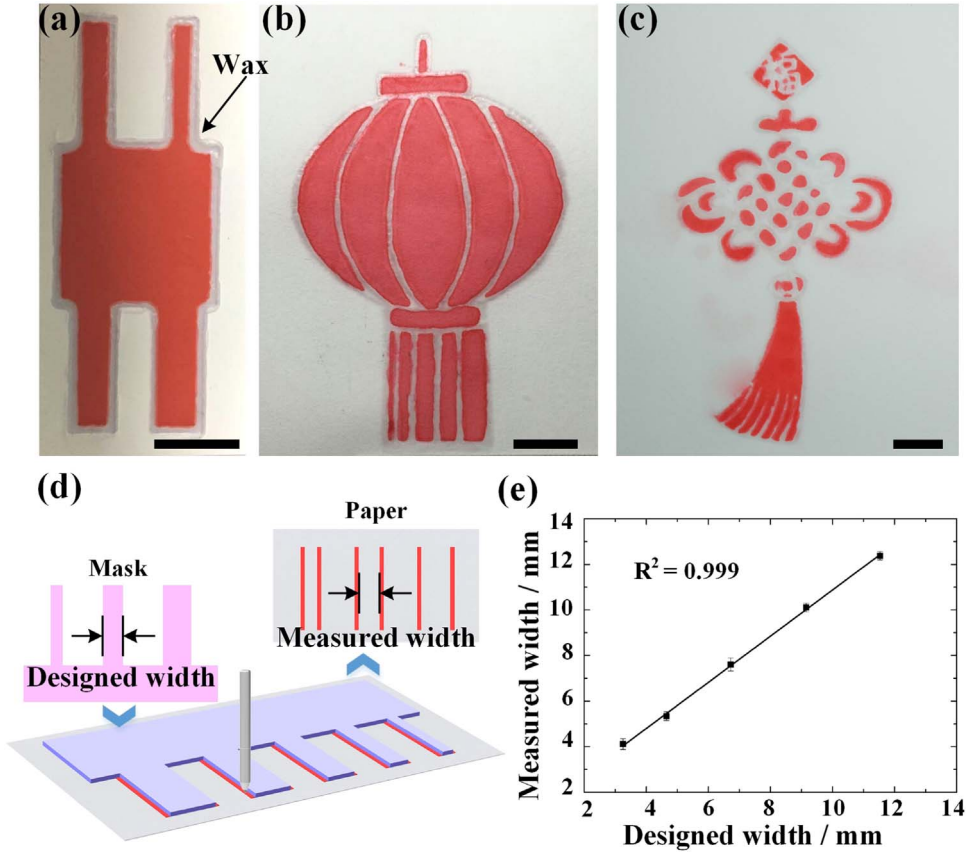

Fig. 3. Pen-on-paper strategy for making microfluidic channels on paper. (a-c) Photographs of a written microfluidic reservoir with four branches, a written lantern and a Chinese knotting filled with red dye (scare bar = 1 cm). (d) Schematic diagram showing the different width of wax channels controlled by using a PMMA mask. (e) The relationship between the measured width of written channels and the designed width of mask.

*target DNA with SSC buffer following the protocol in our previous work (*Tang et al., 2017*).* The glucose solution introduced in electrochemical detection, with concentrations of 1, 5, 10 and 20 mM, was prepared by dissolving the D-(+)-glucose powder into human serum.

3. Results and discussions

3.1. Characterization of the wax pen and the written wax patterns on paper

To evaluate the heating efficiency of the wax pen, we firstly simulated the temperature contour of the axisymmetric section of ball pen in the heating process (Fig. 2). As illustrated in Fig. 2c, the wax cylinder is melted within 5 min, which is rapid enough for the practical utilization. To study the homogeneity of the wax melting process at different positions of the wax pen, six points marked as P1-P6 in the cross section of ball pen were selected (Fig. 2d). We observed that the temperature in the center is lower than the area near the boundary, resulting in a delay in the wax melting process in the center of wax cylinder (P1, P2, P3). The reason is straightforward since the major heat is conducted through the boundary to the center.

The hydrophobic barriers formed inside paper are the key component to construct barrier-defined microfluidic channels on paper. In this work, formation of hydrophobic barriers depends on the penetration of melted wax into the porous paper. To verify the formation of wax barriers inside the paper, we assessed the penetration of the wax after writing by imaging the surface morphology of written wax pattern on paper using scanning electron microscope (SEM, FEI Quanta 250). From the SEM images shown in Fig. 2e, we observed that the melted wax filled in the pores of both NC membrane and filter paper, demonstrating that the hydrophobic wax barriers can be obtained in a one-step manner through writing using the developed wax pen. Besides, the wax patterns on the filter paper are uniform, whereas the patterns on NC membrane are easy to form meniscus mainly due to the low strength of NC membrane. In addition, the ball pen nib contacting the paper under pressure during hand writing leaded to decreased thickness in the middle of written trace on NC membrane. However, this defect poses negligible effect on the fabrication of paper-based microfluidic channels, as explained in the next section.

The liquid wax flows out of the wax pen as the temperature reaches the melting point (~ 50–60 °C), and penetrates into paper in both horizontal and vertical directions. The vertical penetration decides the thickness of the wax pattern and the horizontal penetration decides the width of the wax pattern. Herein, we investigated the influence of temperature on the horizontal penetration of wax, as reflected by the width change of the wax pattern. Fig. 2f shows that the width of the wax pattern increased from 1.30 ± 0.01 mm to 1.60 ± 0.05 mm on NC membrane, and from 1.09 ± 0.03 mm to 1.47 ± 0.03 mm on filter paper when the heating temperature increased from 55 °C to 65 °C. The main reason is that more wax flowed out from the wax pen and penetrated into the paper horizontally with increasing temperature, resulting in the increased width of wax pattern. In addition, the written line on NC membrane was wider than that on filter paper, mainly due to the higher porosity and thinner thickness of NC membrane, which enhance the mass transfer of liquid wax inside the paper along the horizontal direction. Compared to the existing wax patterning methods, this writing method using the developed wax pen is characterized by one-step processing without need for any post-treatment (*e.g.*, heating), thus simplifying the process and reducing energy and time consumption.

3.2. Characterization of the microfluidic channels written on paper

The microfluidic channels on paper are formed by adjacent written

wax lines. To confirm the function of microfluidic channels fabricated by the PoP strategy, a simple microfluidic reservoir with four branches was firstly fabricated on a NC membrane through writing using our wax pen guided by a PMMA mask, which was then loaded with red dye solution (Fig. 3). From the image of the microfluidic reservoir in Fig. 3a, we observed that the red dye solution confined by the wax barrier flows along the branches with different width actuated by capillary force, confirming the full penetration of wax through the paper. Moreover, to further test the capability of our wax pen to write more complicated microfluidic channels on paper, a lantern and a Chinese knot were selected as models and written on filter papers by hand using the wax pen (Fig. 3b-c). We observed that the red dye solution is successfully confined into the microfluidic channels of both lantern and Chinese knot, indicating the versatility of our proposed wax pen-based writing strategy in the fabrication of microfluidic channels on paper. In addition, considering that a designed mask is usually needed during constructing microfluidic channels with precise dimensions, a PMMA mask with five different width was fabricated and used to guide the writing of five different channels on paper (Fig. 3d). The width of channels measured by an optical microscope represent a linear fit to the designed width (Fig. 3e), which demonstrates the feasibility of precisely controlling the sizes of wax patterns by using prepared masks.

3.3. Fully-written paper microfluidic biosensor for Salmonella typhimurium DNA detection

The fabricated paper-based biosensors were further applied in POCT field. Firstly, as inspired from the structure of daily notebooks, we designed and fabricated a paper "notebook" platform for colorimetric detection of *Salmonella typhimurium*, which is a common food-borne pathogen and even may pose permanent damage on human DNA (Miller and Wiedmann, 2016). As shown in Fig. 4a-b, when introducing the sample containing *Salmonella typhimurium DNA* to the inlet of the platform through pipetting, the sample carried with the AuNP-DPs flowed along the wax channel to the detection zone, resulting in a color change on both test and control zones (Fig. 4c-d, Supplemental Video S1). The signal color became deeper as the concentration of *Salmonella typhimurium DNA* increased and no false positive results were observed. The obtained lowest detection limit is 1 nM, which is comparable to those obtained through other methods (*e.g.*, lateral flow strips). Besides, the testing results can be obtained within 5 mins, which is faster than the tests performed on typical lateral-flow assays (LFAs) (~15–30 mins). The reason for this fact may be ascribed to that the fluid flow in the "notebook" design is mainly perpendicular to the paper and thus less flow time on paper "notebook" than lateral fluid flow on the LFAs is consumed. Additionally, the design of the platform, which mimics the working principle of notebook, is not only very simple but also versatile for POCT. For example, it can be easily achieved through designing multi-functional channels for performing multiple assays on paper "notebook". *Specially, in comparison to origami-based 3D paper microfluidic analytical devices (*Li et al., 2013*;* Ma et al., 2015*;* Zang et al., 2012*), the two individual layers of the paper "notebook" can be aligned easily and stacked compactly through only using a spring, which eliminates the need for an external clamp to clamp two layers during folding as used in the origami methods (*Min et al., 2015*). In addition, the liquid flow in the paper "notebook" can be tracked by naked eye as the top layer is transparent.* Furthermore, this "notebook" platform can be extended for multistep assays through employing multiple individual layers with the capability to perform each assay on each layer.

Supplementary material related to this article can be found online at http://dx.doi.org/10.1016/j.bios.2017.06.061.

3.4. Fully-written paper microfluidic biosensor for glucose detection

To verify feasibility of the fully written paper-based biosensor for human health detection, the fabricated paper-based biosensor with

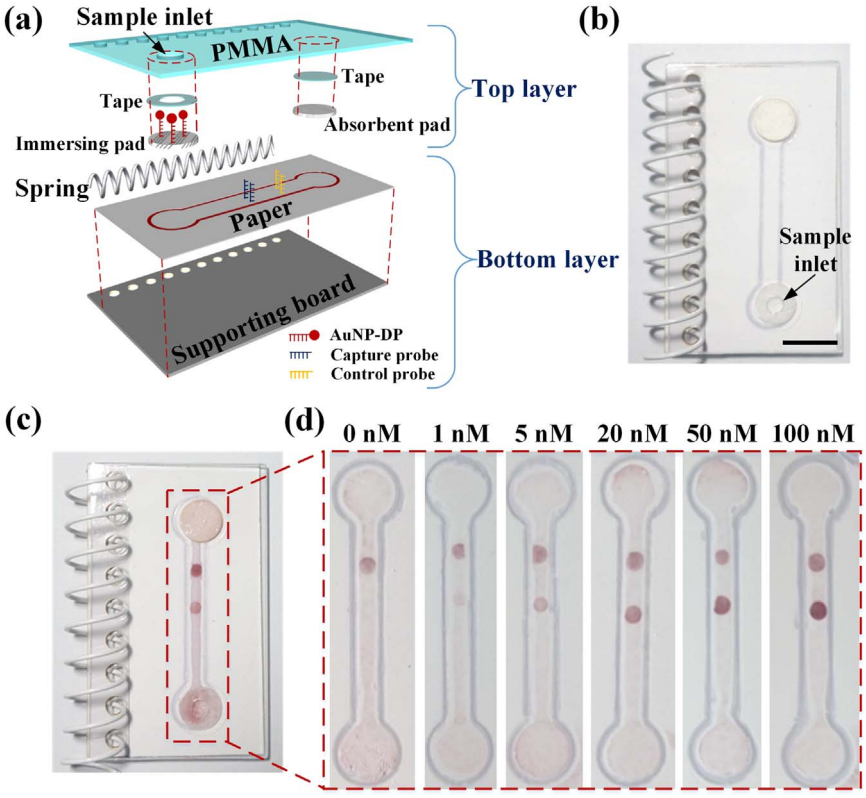

Fig. 4. Pen-on-paper strategy for the colorimetric detection of *Salmonella typhimurium*. (a) The structure of the paper "notebook" platform. (b) Illustration of the folded paper "notebook" platform (scare bar = 1 cm). (c) Photograph showing the color change after sample introduction to the platform. (d) The detection results of *Salmonella typhimurium DNA* with various concentrations.

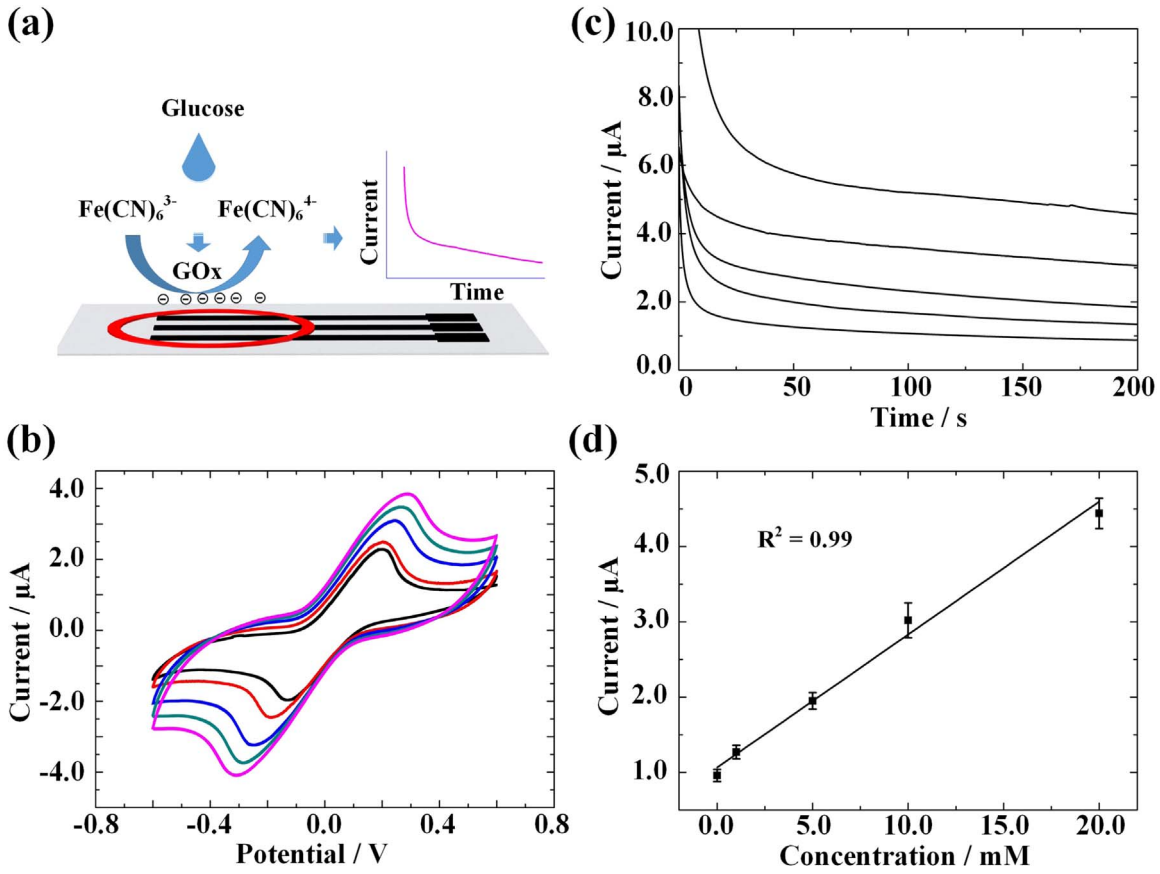

Fig. 5. Pen-on-paper strategy for electrochemical detection of glucose in serum. (a) Schematic of electrochemical biosensors for glucose detection. (b) Cyclic voltammograms of the electrochemical sensors in solution containing 1.0 mM FcMeOH and 0.1 M NaCl at various scan rates (10, 20, 50, 75 and 100 mV s^{-1}). (c) Chronoamperometric curves at the potential of 400 mV for monitoring glucose in spiked serum with concentrations of 0, 1, 5, 10 and 20 mM, respectively. (d) Calibrated current as a function of the concentration of glucose (n = 4).

electrochemical detection unit (*i.e.*, carbon electrodes) was used to detect glucose in human serum, an important index of diabetes (Fig. 5). The fabricated paper-based electrochemical biosensor with a three-electrode system was composed of carbon electrodes and circular microfluidic channel used to restrict sample around the electrodes, *where the wax pen and the ink pen were combined together to write the wax channels and the carbon electrodes, respectively, on the same paper* (Fig. 5a). Prior to glucose testing, the electrochemical performance of the fabricated electrochemical paper-based biosensor was tested by CV measurement with using FcMeOH as the redox mediator. From the obtained cyclic voltammograms in Fig. 5b, a reversible redox behavior of FcMeOH under different scan rates and a ratio of anodic peak current to cathodic peak current (I_{pa}/I_{pc}) of 1.01 on the carbon working electrode of paper-based biosensor were obtained, indicating the good electrochemical performance of the paper-based biosensor. Then from the recorded chronoamperometric curves using the fabricated paper-based biosensor in Fig. 5c, the currents increase with the increase of glucose concentration from 0, 1, 5, 10 to 20 mM in serum. From the calibrated steady-state current, a good linear relationship between the calibrated current and glucose concentration with the detection limit of 1 mM is obtained in Fig. 5d, which is sensitive enough for routine monitoring of glucose, demonstrating the capability of such fully-written paper-based electrochemical biosensor for glucose detection. *The detection results about each measurement using the written biosensor are shown in* Table S3. *The chronoamperometric measurements for detecting glucose with concentration of 1 mM in serum were repeated for four times* (Fig. S1). *The relative standard deviations (RSDs) for each measurement are less than 10%, indicating that the written electrochemical microfluidic biosensor shows good repeatability and accuracy for glucose measurement in real samples.*

4. Conclusions

In this work, we developed a fully written PoP strategy for making paper-based colorimetric and electrochemical POC platforms containing both microfluidic channels and electrodes. The proposed PoP strategy is based on a custom-designed wax pen to write microfluidic channels on paper and a conductive-ink pen to write electrodes on paper. Particularly, our wax pen holds the peculiar capability for one-step fabrication of microfluidic channels on paper by directly penetrating wax into paper during writing without need for any post-treatment. To demonstrate the POCT applications of fabricated paper-based biosensors, we designed a paper-based colorimetric platform mimicking the structure of daily "notebook" for detection of *Salmonella typhimurium DNA* and fabricated a paper-based electrochemical platform for glucose measurement in human serum. The results demonstrate the high practicability of this PoP strategy for both colorimetric and electrochemical POC testing through using the wax pen and conductive-ink pen.

Till now, paper-based microfluidic biosensors have obtained a great development and shown great potential in personalized healthcare fields (Cate et al., 2014). *Even so, there still exist some challenges for realizing self-testing at home, such as the simplicity and commercialization viability of biosensors* (Ahmed et al., 2016). *We believe that our proposed PoP strategy holds great promise for addressing these challenges, as it offers the advantages of true simplicity, rapid prototyping capability, low cost and prominent portability.* However, this proposed PoP strategy mainly relies on hand writing, which is difficult to realize mass production for now. This limitation could be circumvented by integrating the developed pens with programmable two-dimensional plotting platforms. Our further work

would focus on this integration to realize scalable batch manufacturing by using alternative pens loaded with different materials.

Acknowledgements

This work was financially supported by the National Instrumentation Program of China (2013YQ190467), the International Science and Technology Cooperation and Exchange Program of Shaanxi Province of China (2016KW-064), the Fundamental Research Funds for the Central Universities of China (0109-1191320016) and the General Financial Grant from the China Postdoctoral Science Foundation (2016M5927736). The SEM work was done at International Center for Dielectric Research (ICDR), Xi'an Jiaotong University, Xi'an, China.

Appendix A. Supporting information

Supplementary data associated with this article can be found in the online version at doi:10.1016/j.bios.2017.06.061.

References

Abe, K., Suzuki, K., Citterio, D., 2008. Anal. Chem. 80, 6928–6934.
Ahmed, S., Bui, M.-P.N., Abbas, A., 2016. Biosens. Bioelectron. 77, 249–263.
Apilux, A., Dungchai, W., Siangproh, W., Praphairaksit, N., Henry, C.S., Chailapakul, O., 2010. Anal. Chem. 82, 1727–1732.
Bandodkar, A.J., Jia, W., Ramírez, J., Wang, J., 2015. Adv. Healthcare Mater. 4, 1215–1224.
Bruzewicz, D.A., Reches, M., Whitesides, G.M., 2008. Anal. Chem. 80, 3387–3392.
Carrilho, E., Martinez, A.W., Whitesides, G.M., 2009. Anal. Chem. 81, 7091–7095.
Cate, D.M., Adkins, J.A., Mettakoonpitak, J., Henry, C.S., 2014. Anal. Chem. 87, 19–41.
Dornelas, K.L., Dossi, N., Piccin, E., 2015. Anal. Chim. Acta 858, 82–90.
Dossi, N., Toniolo, R., Terzi, F., Impellizzieri, F., Bontempelli, G., 2014. Electrochim. Acta 146, 518–524.
Dungchai, W., Chailapakul, O., Henry, C.S., 2011. Analyst 136, 77–82.
Dungchai, W., Chailapakul, O., Henry, C.S., 2009. Anal. Chem. 81, 5821–5826.
Fenton, E.M., Mascarenas, M.R., López, G.P., Sibbett, S.S., 2008. ACS Appl. Mater. Interfaces 1, 124–129.
Ge, L., Yan, J., Song, X., Yan, M., Ge, S., Yu, J., 2012. Biomaterials 33, 1024–1031.
Hossain, S.M.Z., Brennan, J.D., 2011. Anal. Chem. 83, 8772–8778.
Hossain, S.Z., Luckham, R.E., McFadden, M.J., Brennan, J.D., 2009. Anal. Chem. 81, 9055–9064.
Hu, J., Wang, S., Wang, L., Li, F., Pingguan-Murphy, B., Lu, T.J., Xu, F., 2014. Biosens. Bioelectron. 54, 585–597.
Klasner, S.A., Price, A.K., Hoeman, K.W., Wilson, R.S., Bell, K.J., Culbertson, C.T., 2010. Anal. Bioanal. Chem. 397, 1821–1829.
Li, X., Ballerini, D.R., Shen, W., 2012. Biomicrofluidics 6, 011301–011313.
Li, Z., Li, F., Hu, J., Wee, W., Han, Y., Pingguan-Murphy, B., Lu, T., Xu, F., 2015. Analyst 140, 5526–5535.
Li, W., Li, L., Li, M., Yu, J., Ge, S., Yan, M., Song, X., 2013. Chem. Commun. 49, 9540–9542.
Li, X., Tian, J., Nguyen, T., Shen, W., 2008. Anal. Chem. 80, 9131–9134.
Lu, Y., Shi, W., Jiang, L., Qin, J., Lin, B., 2009. Electrophoresis 30, 1497–1500.
Määttänen, A., Vanamo, U., Ihalainen, P., Pulkkinen, P., Tenhu, H., Bobacka, J., Peltonen, J., 2013. Sens. Actuators, B 177, 153–162.
Ma, C., Li, W., Kong, Q., Yang, H., Bian, Z., Song, X., Yu, J., Yan, M., 2015. Biosens. Bioelectron. 63, 7–13.
Martinez, A.W., Phillips, S.T., Butte, M.J., Whitesides, G.M., 2007. Angew. Chem. Int. Ed. 46, 1318–1320.
Martinez, A.W., Phillips, S.T., Whitesides, G.M., 2008. Proc. Natl. Acad. Sci. USA 105, 19606–19611.
Martinez, A.W., Phillips, S.T., Whitesides, G.M., Carrilho, E., 2009. Anal. Chem. 82, 3–10.
Maxwell, E.J., Mazzeo, A.D., Whitesides, G.M., 2013. MRS Bull. 38, 39–42.
Miller, R.A., Wiedmann, M., 2016. mBio 7, e02109–e02116.
Min, S., Lei, G., Kong, Q., Zheng, X., Ge, S., Li, N., Yu, J., Mei, Y., 2015. Biosens. Bioelectron. 63, 232–239.
Mustaffar, A., Harvey, A., Reay, D., 2015. Appl. Therm. Eng. 90, 1052–1060.
Nie, Z., Deiss, F., Liu, X., Akbulut, O., Whitesides, G.M., 2010a. Lab Chip 10, 3163–3169.
Nie, Z., Nijhuis, C.A., Gong, J., Chen, X., Kumachev, A., Martinez, A.W., Narovlyansky, M., Whitesides, G.M., 2010b. Lab Chip 10, 477–483.
Nie, J., Zhang, Y., Lin, L., Zhou, C., Li, S., Zhang, L., Li, J., 2012. Anal. Chem. 84, 6331–6335.
Nilghaz, A., Wicaksono, D.H., Gustiono, D., Majid, F.A.A., Supriyanto, E., Kadir, M.R.A., 2012. Lab Chip 12, 209–218.
Pardee, K., Green, Alexander A., Takahashi, Melissa K., Braff, D., Lambert, G., Lee, Jeong W., Ferrante, T., Ma, D., Donghia, N., Fan, M., Daringer, Nichole M., Bosch, I., Dudley, Dawn M., O'Connor, David H., Gehrke, L., Collins, James J., 2016. Cell 165, 1255–1266.
Renault, C., Anderson, M.J., Crooks, R.M., 2014a. J. Am. Chem. Soc. 136, 4616–4623.
Renault, C., Koehne, J., Ricco, A.J., Crooks, R.M., 2014b. Langmuir 30, 7030–7036.
Russo, A., Ahn, B.Y., Adams, J.J., Duoss, E.B., Bernhard, J.T., Lewis, J.A., 2011. Adv. Mater. 23, 3426–3430.
Songjaroen, T., Dungchai, W., Chailapakul, O., Laiwattanapaisal, W., 2011. Talanta 85, 2587–2593.
Tang, R., Yang, H., Choi, J.R., Gong, Y., Hu, J., Feng, S., Pingguan-Murphy, B., Mei, Q., Xu, F., 2016. Talanta 152, 269–276.
Tang, R., Yang, H., Gong, Y., You, M., Liu, Z., Choi, J.R., Wen, T., Qu, Z., Mei, Q., Xu, F., 2017. Lab Chip 17, 1270–1279.
Wang, L., Chen, W., Xu, D., Shim, B.S., Zhu, Y., Sun, F., Liu, L., Peng, C., Jin, Z., Xu, C., 2009. Nano Lett. 9, 4147–4152.
Zang, D., Ge, L., Yan, M., Song, X., Yu, J., 2012a. Chem. Commun. 48, 4683–4685.
Zhang, Y., Gao, D., Fan, J., Nie, J., Le, S., Zhu, W., Yang, J., Li, J., 2016. Biosens. Bioelectron. 78, 538–546.